CHARACTERISATION OF CELL MEMBRANE INTERACTION MECHANISMS OF ANTIMICROBIAL PEPTIDES BY ELECTRICAL BILAYER RECORDING

Diana Priyadarshini[1], Josip Ivica[1], Frances Separovic[2], Maurits R. R. de Planque[1]*

[1] Electronics and Computer Science, Faculty of Engineering and Physical Sciences, University of Southampton, Southampton, SO17 1BJ, United Kingdom

[2] School of Chemistry, Bio21 Institute, University of Melbourne, Melbourne, VIC 3010, Australia

*Corresponding author: (e-mail fs@unimelb.edu.au)

ABSTRACT

Many antimicrobial peptides (AMPs) are cationic host defence peptides (HDPs) that interact with microbial membranes. This ability may lead to implementation of AMPs as therapeutics to overcome the wide-spread antibiotic resistance problem as the affected bacteria may not be able to recover from membrane lysis types of attack. AMP interactions with lipid bilayer membranes are typically explained through three mechanisms, *i.e*., barrel-stave pore, toroidal pore and carpet models. Electrical bilayer recording is a relatively simple and sensitive technique that is able to capture the nanoscale perturbations caused by the AMPs in the bilayer membranes. Molecular-level understanding of the behaviour of AMPs in relation to lipid bilayers mimicking bacterial and human cell membranes is essential for their development as novel therapeutic agents that are capable of targeted action against disease causing micro-organisms. The effects of four AMPs (aurein 1.2, caerin 1.1, citropin 1.1 and maculatin 1.1 from the skin secretions of Australian tree frogs) and the toxin melittin (found in the venom of honeybees) on two different phospholipid membranes were studied using the electrical bilayer recording technique. Bilayers composed of zwitterionic (DPhPC) and anionic (DPhPC/POPG) lipids were used to mimic the charge of eukaryotic and prokaryotic cell membranes, respectively, so as to determine the corresponding interaction mechanisms for different concentrations of the peptide. Analysis of the dataset corresponding to the four frog AMPs, as well as the resulting dataset corresponding to the bee toxin, confirms the proposed peptide-bilayer interaction models in existing publications and demonstrates the importance of using appropriate bilayer compositions and peptide concentrations for AMP studies.

KEYWORDS

Antimicrobial peptides, bilayer lipid membranes, lipid-peptide interactions, phospholipids

INTRODUCTION

Antimicrobial peptides (AMPs) are small proteins produced by the immune systems of complex living organisms. Also known as host defence peptides (HDPs), these molecules are known to protect the host cells from infectious diseases caused by micro-organisms. Over the past few decades, AMPs found in the secretions of certain species of frogs, bees and scorpions in particular, have been studied for their ability to destroy microbes or cancer cells, potentially by rupturing the phospholipid bilayer of the target cell membranes. Deeper understanding of these peptide-membrane interactions can lead to the development of a novel class of drugs which potentially is unaffected by the prevalent issue of antibiotic resistance [1].

Three generally accepted models that are used to explain the mechanisms of interaction between AMPs and bilayer membranes are considered here. Following adsorption onto the lipid layer, the AMPs perturb the membrane by inducing toroidal or barrel-stave pores or defragment the entire membrane in a carpet-like mechanism [2][3]. Depending on factors such as temperature, peptide concentration, lipid environment, duration of exposure, etc., the same AMP may exhibit one or a combination of these interaction mechanisms with respect to the bilayer membrane. In this study, these models for the action of AMPs were investigated through electrophysiology experiments and analyses of the resulting high-resolution peptide-mediated current traces in phospholipid bilayers [4].

Step-like currents showing orthogonal jumps and plateaus are usually associated with barrel-stave pores, where transmembrane peptides are tightly bound together around a central opening, whereas multi-level currents showing jumps with fluctuations are mainly attributed to the formation of toroidal pores, where the pore size varies depending on the surrounding lipid interaction with the peptides. Erratic currents showing rapid and clustered fluctuations are associated with the carpet model, where peptides cover the lipid membrane surface in random clusters, eventually forming transmembrane pores and disintegrating the bilayer in a detergent fashion. Finally, spikey currents that show short duration isolated fluctuations indicate instantaneous defects in the bilayer membrane caused by the permeation of peptides and can be considered as a separate ‘penetration’ model or as a part of the relevant transmembrane pore models [5-9].

Electrical recording of the interaction of melittin peptides with suspended lipid bilayer structures formed at a microfabricated Teflon aperture have been employed previously [7]. The technique is able to record single molecule perturbations in the nanometre range. Due to its high sensitivity and simplicity compared to other advanced characterisation techniques, we have used it to study four AMPs found in the skin secretion of Australian tree frog species: aurein 1.2, caerin 1.1, citropin 1.1 and maculatin 1.1, and the lytic peptide, melittin found in European honeybee venom [10-12]. These five membrane-active peptides were studied in self-assembled bilayers made up of synthetic phospholipids DPhPC (1,2-diphytanoyl-sn-glycero-3-phosphocholine) [4] and mixed with POPG (1-palmitoyl-2-oleoyl-phosphatidylglycerol) DPhPC/POPG (4:1 w/w) [13] to mimic the charge of human and bacterial cell membranes, respectively. The resulting current traces of the peptides at

various concentrations and voltages were analysed to corroborate the mechanism by which the corresponding AMPs interact with the two different types of bilayer membranes.

MATERIALS AND METHODS

Equipment

The electrical recording experimental set up for the phospholipid bilayer membrane is mainly composed of two Teflon chambers screwed together with a Teflon aperture sheet in between, supported by an acrylic platform placed on an electromagnetic base and housed in a Faraday cage (Warner Instruments, Holliston, MA, USA) enclosure which is appropriately grounded to provide electromagnetic shielding for the sensitive electronics inside [14][15]. Teflon is usually the material of choice for both the aperture film and the bilayer chamber due to its durability, machinability, resistance to solvents and low contribution to excess noise levels when exposed to salt solutions during bilayer formation and recordings [16][17]. The Ag/AgCl microelectrodes connected to *cis* (left) and *trans* (right) sides of the recording chamber act as cathode and anode terminals of an electrochemical cell. In our system, the grounded Ag/AgCl electrode was in the *cis* chamber and the membrane voltage was set by the electrode placed in the *trans* chamber. The signals are amplified and digitised, and the resulting signal is displayed on the computer using Clampex 10.4 (Molecular Devices).

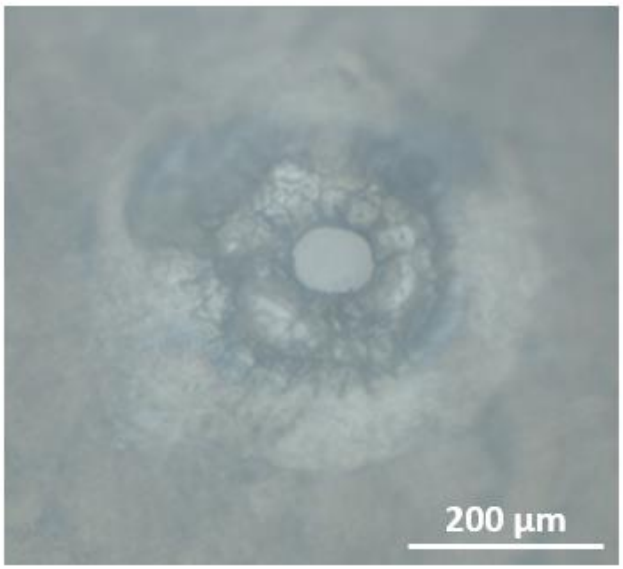

Fig. 1: Microscopic image of the circular aperture in the Teflon film square viewed under objective lens with 10x magnification, showing smooth and uninterrupted boundaries formed through laser ablation.

The Teflon aperture shown in Fig. 1 measured approximately 83.2 µm in diameter and 261.4 µm in circumference, which allows the formation of a bilayer membrane with low background current noise and capacitance [17]. Considering that the lipid bilayer formed across this aperture has a thickness of 5 nm [18] and relative dielectric constant of 2.5 [19], its capacitance value can be estimated as 24.1 pF, which is the value expected for the

corresponding output signal representing a stable bilayer. This 'open chamber' configuration of bilayer recording, which involves the formation of a lipid bilayer membrane over an aperture in a partition separating two chambers containing electrolytes, offers greater flexibility of operation and minimizes the background current noise [16][17].

Reagents and Chemicals

Unless specified otherwise, all the chemicals used are from Sigma-Aldrich (Merck Life Sciences, Gillingham, UK).

Buffer or electrolyte solution was prepared using potassium chloride (KCl) from Fisher Scientific, ethylenediaminetetraacetic acid (EDTA) from Melford Biolaboratories and tris(hydroxymethyl) aminomethane (THAM or Trizma®) base mixed in deionized (DI) water. This mixture of salt, weak acid and strong base at concentrations of 1 M, 1 mM and 10 mM, respectively, was balanced using hydrochloric acid (HCl) at a concentration of 1 M to maintain the buffer solution close to the physiological level of pH 7.8 [18]. The high salt concentration was also essential to minimise the access resistance of the electrolyte solution and free movement of K^+ ions across the perforated bilayer membrane at the aperture separating the two chamber halves [16][17].

Primer solution consisting of 10 µl of n-hexadecane (99%, pure) from Acros Organics was mixed with 190 µl of n-hexane (95%, anhydrous). This non-polar organic solution was used to treat the Teflon film for supporting and enhancing the bilayer formation at its aperture, resulting from the two self-assembled monolayers (SAMs) of the amphipathic lipid molecules [20].

Lipid solution was prepared using DPhPC (1,2-diphytanoyl-sn-glycero-3-phosphocholine) from Avanti Polar Lipids dissolved in an organic solvent (typically chloroform) for short term use and stable storage. Required lipid quantity of 20 mg was mixed with 1 ml of chloroform to make up 20 mg/ml concentration of the lipid sample. Similarly, a combination of DPhPC/POPG lipids in the ratio of 4:1 w/w (or 3.66:1 mole/mole) was prepared by mixing 16 mg of DPhPC and 4 mg of POPG (1-palmitoyl-2-oleoyl-phosphatidylglycerol), also from Avanti, with 1 ml of chloroform to make up another 20 mg/ml concentration of lipid sample.

Peptide solution was prepared using melittin (product code M2272) dissolved in an organic solvent, e.g. dimethyl sulfoxide (DMSO) as reported [7][21]. Considering the toxicity levels of the solvent and minimum quantity limitations of the electronic balance, 1 mg of melittin was dissolved in a low volume of 200 µl of DMSO to get 1.757 mM concentration for the peptide sample. This was then diluted to give a stock solution of 100 µM concentration of melittin in DMSO.

Similar AMP samples were prepared by individually dissolving the peptides, aurein 1.2, caerin 1.1, citropin 1.1 and maculatin 1.1, in water-based buffer solution containing 1 M of KCl and 10 mM of 4-(2-hydroxyethyl)piperazine-1-ethanesulfonic acid (HEPES) at pH 7.4 for the respective AMP-bilayer recordings.

Procedure

Bilayer currents were measured with an Axopatch 200B amplifier (Molecular devices) in the whole-cell (β=1 configuration). The current output was limited to the+/-1000 pA range with the gain of the amplifier set to 10x. Current crossing this threshold was considered as the bilayer rupture. Membrane was voltage-clamped and the currents were prefiltered with the 10 kHz low-pass Bessel filter (built in the amplifier). The currents were sampled at 50 kHz with an Digidata 1440A (Molecular Devices) and stored on a computer hard drive with the Clampex 10.2 software (Molecular Devices).

As the solution levels in the bath chambers were gradually lowered and raised, the lipid molecules which were initially positioned in a heads-down configuration on the liquid surface, came together to form a lipid bilayer membrane at the aperture due to hydrophobic interactions, as previously described [22]. This bilayer lipid membrane at the aperture prevents the flow of ions across the two chamber halves, resulting in a drastic drop in current and capacitance levels from values beyond the recording range down to almost zero. As the peak amplitude value of this capacitive square wave, i.e., +/- 30 pF was close to the estimated value of 24.1 pF, this output signal indicates the presence of a stable lipid bilayer at the Teflon aperture.

Once the stability of the bilayer was confirmed, the recording of the output current trace was begun and the peptide was introduced, starting with the lowest concentration, into the *cis* side of the chamber. Any perturbations caused by the peptide on the bilayer membrane were recorded using the software and manifested as increased amplitude levels in the output current trace. Later, a new recording was initiated and additional volumes of higher concentrations of the peptide solution were sequentially added. Input voltage was changed to different values, such as +/- 100 mV, 120 mV, 80 mV and 50 mV throughout the recording session, to observe the corresponding changes in the output current traces. Each recording session was continued until the current amplitude fell back to the baseline level or until the bilayer broke, and the new recording begun after bilayer re-formation but before the addition of the next peptide volume.

These steps were repeated by forming the bilayer using the DPhPC/POPG (4:1 w/w) lipid combination. Resulting output files corresponding to all five peptides were additionally filtered with a low-pass Gaussian 5 kHz (software filter) and analysed to better understand their mechanisms of interaction with the two different types of model membranes.

RESULTS AND DISCUSSION

Initial Observations

The minimum inhibitory concentration for AMps is typically in the μM range [7] and, although an AMP would not interact act in the same way with a phospholipid membrane bilayer, we studied the five peptides at different concentrations in the range of 0.1 μM to 40 μM. As described above, Clampfit 10.7 software (Molecular Devices) was used to analyse a total of 140 output files each ranging from tens of seconds up to almost two hours in duration of recording with DPhPC and DPhPC/POPG (4:1 w/w) bilayer membranes under the application of several voltages ranging from -150 mV to +150 mV. However, considering the

transmembrane potential value, which is usually below 0.1 V for most animal cells [17], this section is primarily focused on current traces recorded at 100 mV voltage. A screenshot of one of the recording files is shown in Fig. S1 in Supplementary Information (SI) to present the overall view of a typical reference analysis sample.

As the traces were recorded at a high low pass filter cut-off frequency of 10 kHz (Bessel filter) set in the hardware during the experiments, software filter settings were used to remove unwanted background noise from the required output trace. Hence, for the purpose of the analysis, current traces were additionally filtered with an 5kHz low-pass Gaussian filter in Clampfit 10.7 (Molecular Devices)

Qualitative Analysis

Analyses of selected current trace sections corresponding to the interaction of the five peptides with the two types of lipid bilayers are summarised by the graphs in Fig. 2 for aurein 1.2 against the two types of lipid bilayers. Constituent data points were extracted from particular trace sections and plotted using a common viewing scale for comparison of the various peptide-lipid combinations.

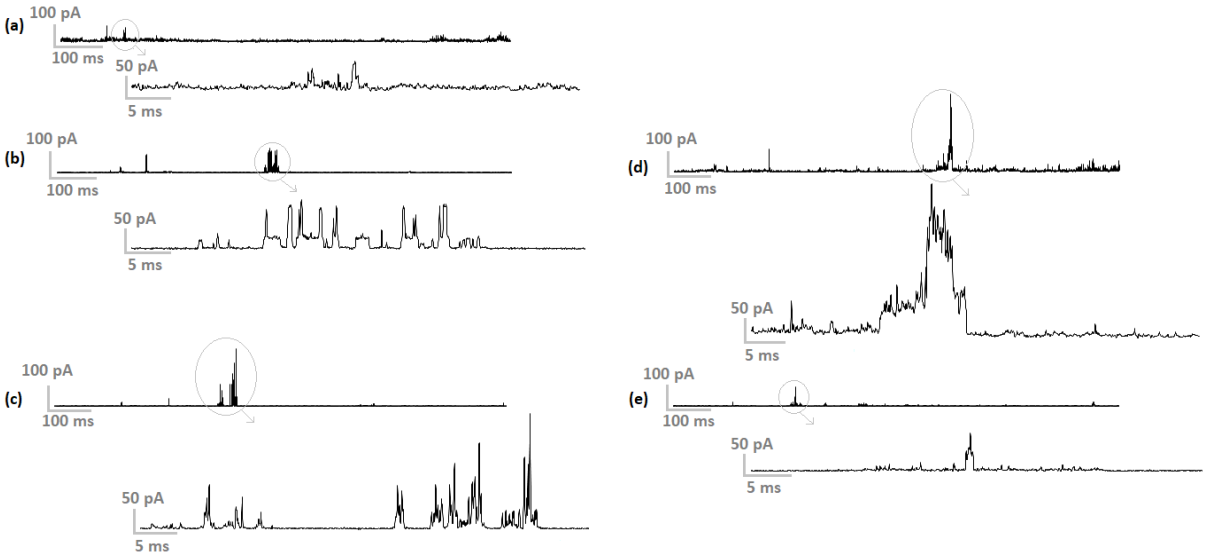

Fig. 2: Current vs. time plots representing the action of aurein 1.2 at approximate concentrations of: (a) 0.1 µM, (b) 1 µM, and (c) 10 µM on DPhPC bilayer, as well as (d) 1 µM, and (e) 10 µM on DPhPC/POPG (4:1) bilayer, recorded over a duration of 1 s. Corresponding magnified views of specific features for a 50 ms duration are also included.

At the concentration of 0.1 µM against a DPhPC bilayer, aurein 1.2 showed wide spikes with amplitudes in the range of 70 pA and increased baseline current level at about 20 pA, whereas at higher concentrations of 1 µM and 10 µM against the same bilayer, it showed taller spikes in the range of 120 pA with wider base, similar to a raised platform or step with spikes on top, but with the baseline level back at 0 pA. Similar but more prominent features were observed against DPhPC/POPG (4:1) bilayers but with less frequency.

Caerin 1.1 against both DPhPC and DPhPC/POPG (4:1) bilayers produced a largely ‘spike signal’ behaviour in comparison to aurein 1.2 and with more prominent effect as the

peptide concentration was increased (see Fig. S2 in SI). Although some step-like features were observed for the DPhPC traces, baseline level remained at 0 pA in all cases except for the trace corresponding to caerin concentration at 0.1 µM against DPhPC/POPG bilayer where the current baseline increased up to 5 pA level. Moreover, at high peptide concentrations of 10 µM against DPhPC/POPG bilayer, peak amplitudes exceeded the upper limit of 1000 pA set in the hardware and resulted in bilayer breakdown.

The behaviour of citropin 1.1 (Fig. S3, SI) was quite similar to that of aurein 1.2, showing step-like features with sharp spikes on top for both bilayer types and all three peptide concentrations. Baseline current level was also higher than 0 pA for all cases except for citropin concentration of 10 µM against pure DPhPC bilayer.

The action of maculatin 1.1 (Fig. S4, SI) was more similar to that of caerin 1.1 than aurein 1.2 or citropin 1.1, showing predominantly spikey signal behaviour against both pure and mixed DPhPC bilayers. Baseline current was ~10 pA or more for all cases except for 1 µM concentration of maculatin against DPhPC bilayer where it was at the usual 0 pA level. Although the amplitude of the spikes did not cross the hardware set limit of 1000 pA, their frequency is clearly higher than those observed in the caerin traces.

On the other hand, melittin from bee venom behaves very differently as seen in Fig. 3, compared to the four AMPs found in frog skin secretions. Particularly for the traces of 0.1 µM and 1 µM melittin concentrations against pure DPhPC bilayer, distinct steps with almost perfect vertical separation of about 15 pA between the higher and lower current levels were clearly visible.

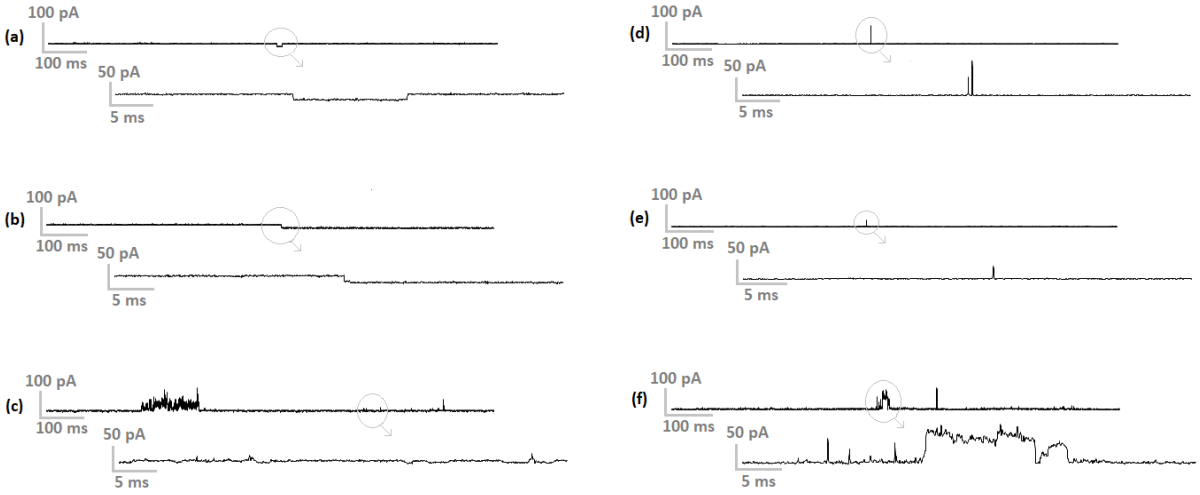

Fig. 3: Current vs. Time plots representing the action of melittin at approximate concentrations of (a) 0.1 µM, (b) 1 µM and (c) 10 µM on DPhPC bilayer, as well as (d) 0.1 µM, (e) 1 µM and (f) 10 µM on DPhPC/POPG (4:1) bilayer, recorded over a duration of 1 s. Corresponding magnified views of specific features for a 50 ms duration are also included.

Baseline current level was in the range of 10 pA for all melittin cases, with the exception of 0.1 µM and 1 µM concentrations against DPhPC/POPG (4:1) bilayer where it was at the usual 0 pA level. Also, spikey signal behaviour was observed for these two traces but with low amplitudes of around 50 pA and very low frequency with only 1 or 2 spikes. Higher

concentrations of 10 µM melittin caused both spikes and step-like behaviours for both types of lipid bilayers with higher frequencies and peak amplitudes reaching up to ~120 pA.

Considering the variations in the feature shapes throughout the duration of voltage application, the current traces were also analysed based on the occurrence of the four prominent pattern types over each 1 s duration and the results were plotted in the form of doughnut plots as shown in Fig. 4.

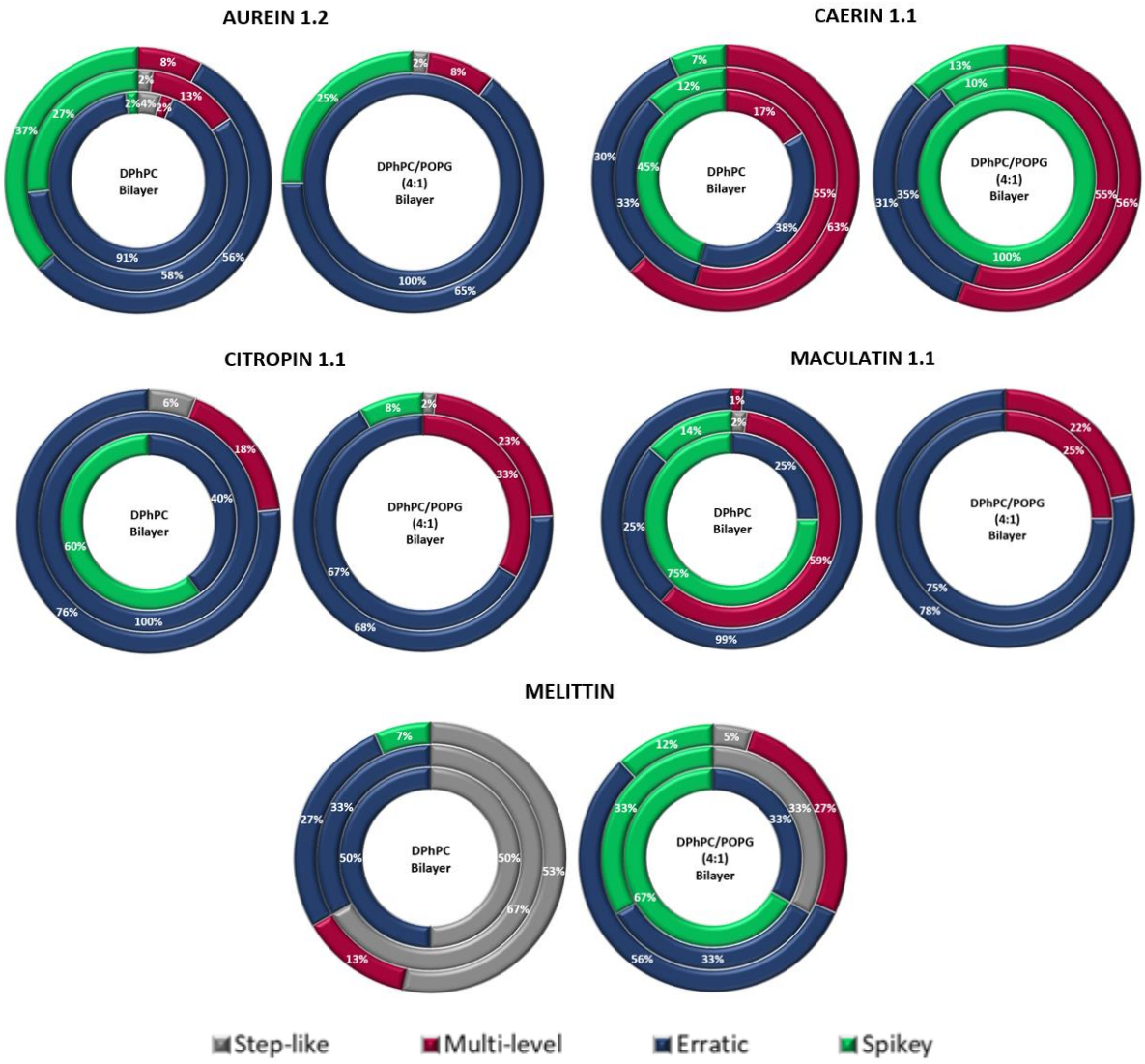

Fig. 4: Approximate percentage distribution of the four prominent signal types in the current traces of the four AMPs, aurein 1.2, caerin 1.1, citropin 1.1 and maculatin 1.1, and the toxin melittin against DPhPC and DPhPC/POPG (4:1) bilayers. The innermost ring represents 0.1 µM, middle ring 1 µM and outermost ring 10 µM peptide concentrations. Plots with only two rings represent peptide concentrations of 1 µM (inner ring) and 10 µM (outer ring) only.

For the plots in Fig. 4, 'spikey' signals are considered as isolated peaks which rise from and fall back to the baseline level within short durations of up to 20 ms each, while 'erratic' signals are considered as clusters of peaks which occur for durations of 20 ms or more

without forming any distinct shapes as such. ‘Multi-level’ signals are similar to erratic signals but usually have vertical rises and falls in the current levels in relation to the baseline level, ranging from 20 ms to 200 ms in time duration, and are mostly isolated. Lastly, the ‘step-like’ signals are identified by their distinctive orthogonal current jumps with respect to the baseline level without any peaks at either the bottom or top levels [23]. Almost all the plots of Fig. 4 show a combination of these four prominent signal features in various proportions depending on the peptide concentrations (with 0.1 µM corresponding to the innermost ring, 1 µM corresponding to the middle ring and 10 µM corresponding to the outermost ring) and the type of bilayer involved (with pure DPhPC on the left-hand side and DPhPC/DOPG on the right-hand side plots). We were unable to collect sufficient recordings for analysis from the shorter peptides at 0.1 µM concentration with DPhPC/DOPG as the bilayers are fragile and frequently burst over the longer time period required to observe activity. However, the longer peptides caerin 1.1 and melittin showed greater activity and data for the anionic bilayers are shown in Fig. 4.

Quantitative Analysis

Analysis of selected current trace sections corresponding to the interaction of the five peptides with the two types of lipid bilayers is summarised in Table 1 and Figure 6. The data are at 100 mV and 5 kHz Gaussian low pass filter, with the exceptions of citropin 1.1 and maculatin 1.1 with DPhPC/POPG which are at 50 mV as the bilayers were more stable for a longer period. A single ‘event’ represents a portion of the trace where the current amplitude rose above the specified ‘trigger level’ as shown in Fig. S5 of SI. Peptide activity in the bilayer was investigated with the threshold search protocol with Clampfit 10.4 software (Molecular Devices). The threshold level was set to 10 pA in order to exclude smaller current perturbations in the bilayer from the analysis. Event Frequency was calculated as Event Count divided by the Time Duration of Voltage Application. All five peptides at different concentrations were evaluated in relation to the frequency of events parameter, which represents their activity levels against the two bilayer membrane types as shown in Fig. 5.

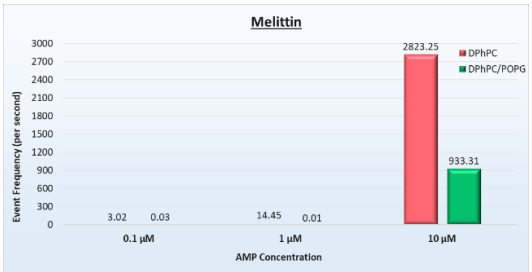

Fig. 5: Event Frequency vs. Peptide Concentration for the five peptides at three different concentration levels. Red are for DPhPC while green bars are for DPhPC/POPG bilayers.

At the concentration of 1 µM, the AMPs aurein 1.2, caerin 1.1 and citropin 1.1 were more active against DPhPC/POPG (4:1) bilayers, which represent prokaryotic cell membranes. However, at 10 µM concentration, only citropin 1.1 and maculatin 1.1 were more active against DPhPC/POPG (4:1) bilayers, compared to DPhPC bilayers which represent eukaryotic cell membranes. Also, at all three specified concentrations, melittin was three times more active against DPhPC bilayers compared to DPhPC/POPG (4:1) bilayers, which suggests that the toxin can cause more damage to eukaryotic cells than to microbes.

Summary of Analyses

Analysis of the results obtained from both the qualitative and quantitative approaches, and the prominent signal feature distribution plots of Fig. 4 in particular, the following peptide-membrane interaction models are proposed and summarized in Table 1.

Although the current traces include all the four signal shapes described in this report, only the dominant behaviour observed for each AMP-bilayer-concentration combination was considered so as to determine the corresponding interaction mechanism. It is based on the typical associations of step-like signals with the barrel-stave pore model, multi-level signals with a toroidal pore model and erratic signals with the carpet model. Spikey signals were mostly ignored based on the assumption that they represent minor bilayer perturbations caused by insignificant movement of the peptides. The toroidal pore model is proposed for caerin 1.1 at a concentration of 0.1 µM against DPhPC bilayer, despite the higher percentage of erratic signals, because of the absence of membrane rupture; while a carpet model is proposed for melittin at a concentration of 10 µM against DPhPC bilayed due to the occurrence of membrane rupture which is usually expected for the carpet model and associated with these signal features. In general, the proposed interaction models for 0.1 µM of caerin 1.1 and maculatin 1.1 against pure DPhPC as well as melittin at all three concentrations against DPhPC/POPG can be inter-changed between toroidal pore and carpet type based on the similarity of their respective signal distribution percentages and difficulty in distinguishing between different models for these cases.

Table 1: The five peptides and the mechanism proposed for their interactions with neutral and anionic phospholipid bilayers at three different peptide concentrations.

Peptide	**Bilayer**	**Interaction Model**		
		0.1 µM	**1 µM**	**10 µM**
Aurein 1.2	DPhPC	Carpet		

	DPhPC/POPG (4:1)	-	Carpet	
Citropin 1.1	DPhPC	Carpet		
	DPhPC/POPG (4:1)	-	Carpet	
Maculatin 1.1	DPhPC	Carpet	Toroidal Pore	Carpet
	DPhPC/POPG (4:1)	-	Carpet	
Caerin 1.1	DPhPC	Toroidal Pore		
	DPhPC/POPG (4:1)			
Melittin	DPhPC	Barrel-Stave Pore		
	DPhPC/POPG (4:1)	Carpet		

These results and interpretations are consistent with the models proposed in related publications by Separovic and coworkers [1][24-28] and Fennouri *et al.* [7], except for the case of melittin where barrel-stave or toroidal pore models are usually observed [29]. The four AMPs from Australian tree frogs have similar chemical and structural properties. Aurein 1.2, citropin 1.1, maculatin 1.1 and caerin 1.1 contain 13, 17, 21 and 25 amino acid residues in their respective chains, along with amidated (-NH_2) C-termini and overall positive charge values. On the other hand, melittin which is found in bee venom, is a comparatively longer peptide containing 26 amino acid residues [30] and is more highly charged (+6). Its short peptide chain length limits aurein 1.2 interaction with the bilayers to the carpet mechanism, while the other peptides, due to their longer amino acid sequences, are more capable of spanning the bilayer thickness of 5 nm and can interact through pore or non-pore mechanisms depending on factors such as peptide concentration, bilayer lipid composition and environmental conditions [31-34]. While all five peptides exhibit affinity for lysing bacterial membranes, melittin in particular has lytic tendencies towards membranes made of neutral lipids, due to its comparatively high cationic charge and low hydrophobicity values, which correlates with its cytotoxic effect on human cells [7][30][34][35]. Also, melittin exhibits both pore and non-pore behaviours with DPhPC/POPG bilayer due to the competing reactions of direction insertion into the zwitterionic membrane and surface interaction with the PG lipid head groups [36].

Overall, AMPs as membrane-active cationic host defence peptides [37] are expected to assemble themselves to form either transmembrane pores, that may eventually close, or aggregates that accumulate on the bilayer surface. These mechanisms may continue to occur independently or in combination until membrane destabilisation and eventual rupture is achieved due to the impact on the structural integrity of the bilayer [24][30]. The observation of signal features corresponding to both toroidal pore and carpet models in the same current trace supports this proposition. However, we also note that minimum inhibitory concentration values of AMPs tend to be in the low micromolar range [38], which is somewhat higher than conventional small-molecule antibiotics [39]. At such growth-inhibiting concentrations, bacterial membranes could be completely covered by AMPs [40]. In the absence of lysis or permeabilisation, it cannot be ruled out that electrical bilayer recordings capture the effects of bilayer translocation and that AMPs have intracellular targets [37][41].

CONCLUSION

In summary, analysis of the electrical bilayer recordings for the selected peptide-bilayer combinations reveals that aurein 1.2, citropin 1.1 and maculatin 1.1 predominantly exhibit carpet mechanism against DPhPC as well as DPhPC/POPG (4:1) lipid bilayer membranes, while the longer AMP, caerin 1.1, predominantly exhibits a toroidal pore mechanism against both types of membranes. Melittin interacts with the pure DPhPC bilayer mainly through the barrel-stave pore mechanism and with the anionic bilayer primarily through the carpet mechanism. Considering their respective activity and affinity levels towards the two types of bilayer membranes, aurein 1.2, citropin 1.1, maculatin 1.1 and caerin 1.1 seem better suited for disturbing microbial membranes while melittin seems more suitable for disrupting eukaryotic membranes.

The electrical bilayer recording data and the corresponding results obtained herewith could be further evaluated to determine parameters such as size of the bilayer pores, number of peptide monomers involved in the pore formation, minimum inhibitory concentration, etc., in relation to peptide-membrane interactions [22][42][43]. Also, the experimental setup could be automated using droplet microfluidic systems, including lipid bilayer formation and transmembrane current measurement, resulting in increased throughput assays [44][45].

SUPPORTING INFORMATION

Supplemental Information, including output current trace of 1 µM aurein 1.2 on DPhPC/POPG bilayer membrane; current vs. time plots of caerin 1.1, citropin 1.1 and maculatin 1.1 on bilayer lipid membranes; and sample trace showing the Threshold Search option of the Clampfit software; can be found with this article.

ACKNOWLEDGEMENTS

The authors would like to acknowledge Ruoyu Hu, University of Southampton, for his help with the melittin recordings. F.S. would like to thank the Bio21 Peptide Facility for synthesis of the antimicrobial peptides and the University of Southampton for hosting her sabbatical visit during which this work was started.

REFERENCES

[1] E. E. Ambroggio, F. Separovic, J. H. Bowie, G. D. Fidelio, and L. A. Bagatolli, “Direct Visualization of Membrane Leakage Induced by the Antibiotic Peptides: Maculatin, Citropin, and Aurein”, Biophysical Journal, vol. 89 (3), 2005, pp. 1874-1881.

[2] J. Li, J.-J. Koh, S. Liu, R. Lakshminarayanan, C. S. Verma, and R. W. Beuerman, “Membrane Active Antimicrobial Peptides: Translating Mechanistic Insights to Design”, Frontiers in Neuroscience, vol. 11, 2017, p. 73.

[3] A. Giuliani, G. Pirri, A. Bozzi, A. Di Guillo, M. Aschi, and A. C. Rinaldi, “Antimicrobial peptides: natural templates for synthetic membrane-active compounds”, Cellular and Molecular Life Sciences, vol. 65 (16), 2008, pp. 2450-2460.

[4] T. Baba, Y. Toshima, H. Minamikawa, M. Hato, K. Suzuki, and N. Kamo, “Formation and characterization of planar lipid bilayer membranes from synthetic phytanyl-chained glycolipids”, Biochimica et Biophysica Acta (BBA) – Biomembranes, vol. 1421 (1), 1999, pp. 91-102.

[5] M. Aquila, M. Benedusi, A. Milani, and G. Rispoli, “Enhanced Patch-Clamp Technique to Study Antimicrobial Peptides and Viroporins, Inserted in a Cell Plasma Membrane with Fully Inactivated Endogenous Conductances”, in “Patch Clamp Technique”, F. S. Kaneez (Ed.), IntechOpen, 2012, p. 332, [Online]. Available: https://www.intechopen.com/chapters/33642

[6] Y. Sekiya, S. Sakashita, K. Shimizu, K. Usui, and R. Kawano, “Channel current analysis estimates the pore formation and the penetration of transmembrane peptides”, Analyst, vol. 143 (15), 2018, pp. 3540-3543.

[7] A. Fennouri, S. F. Mayer, T. B. H. Schroeder, and M. Mayer, “Single channel planar lipid bilayer recordings of the Melittin variant MelP5”, Biochimica et Biophysica Acta (BBA) – Biomembranes, vol. 1859 (10), 2017, pp. 2051-2057.

[8] C.-F. Le, C.-M. Fang, and S. D. Sekaran, “Intracellular Targeting Mechanisms by Antimicrobial Peptides”, Antimicrobial Agents and Chemotherapy, vol. 61 (4), 2017, e02340-16.

[9] H. Sato, and J. B. Feix, “Peptide-membrane interactions and mechanisms of membrane destruction by amphipathic α-helical antimicrobial peptides”, Biochimica et Biophysica Acta (BBA) – Biomembranes, vol. 1758 (9), 2006, pp. 1245-1256.

[10] M. T. Tosteson, and D. C. Tosteson “The sting. Melittin forms channels in lipid bilayers”, Biophysical Journal, vol. 36 (1), 1981, pp. 109-116.

[11] C. E. Dempsey, R. Bazzo, T. S. Harvey, I. Syperek, G. Boheim and I. D. Campbell, “Contribution of proline-14 to the structure and actions of melittin”, FEBS Letters, vol. 281, 1991, pp. 240-244.

[12] S. Stankowski, M. Pawlak, E. Kaisheva, C. H. Robert, and G. Schwarz, “A combined study of aggregation, membrane affinity and pore activity of natural and modified melittin”, Biochim Biophys Acta, vol. 1069, 1991, pp. 77-86.

[13] J. T. J. Cheng, J. D. Hale, M. Elliott, R. E. W. Hancock, and S. K. Straus, “The importance of bacterial membrane composition in the structure and function of aurein 2.2 and selected variants”, Biochimica et Biophysica Acta (BBA) – Biomembranes, vol. 1808 (3), 2011, pp. 622-633.

[14] “BC-535 Manual (060126)”, Warner Instruments LLC, Connecticut, United States of America, 2018, [Online]. Available: https://www.warneronline.com/introduction-to-the-blm-workstation

[15] “Introduction to BLM Workstation”, Warner Instruments LLC, Connecticut, United States of America, 2018, [Online]. Available: https://www.warneronline.com/two-electrode-voltage-clamp-workstation-tev-700

[16] W. F. Wonderlin, A. Finkel, and R. J. French, “Optimizing planar lipid bilayer single-channel recordings for high resolution with rapid voltage steps”, Biophysical Journal, vol. 58 (2), 1990, pp. 289-297.

[17] “Axon Guide to Electrophysiology and Biophysics Laboratory Techniques”, 3rd ed., Molecular Devices LLC, California, United States of America, 2012, [Online]. Available: https://www.moleculardevices.com/en/assets/user-guide/dd/cns/axon-guide-to-electrophysiology-and-biophysics-laboratory-techniques

[18] D. L. Nelson, and M. M. Cox, “Lehninger Principles of Biochemistry”, 5th ed., W. H. Freeman and Company, 2008, pp. 362 and 373.

[19] S. Ohki, “Dielectric constant and refractive index of lipid bilayers”, Journal of Theoretical Biology, vol. 19 (1), 1968, pp. 97-115.

[20] P. Bartsch, C. Walter, P. Selenschik, A. Honigmann, and R. Wagner, “Horizontal Bilayer for Electrical and Optical Recordings”, Materials, vol. 5 (12), 2012, pp. 2705-2730.

[21] Y.-X. Tan, C. Chen, Y.L. Wang, S. Lin, Y. Wang, S.-B. Li, X.-P. Jin, H.-W. Gao, F.-S. Du, F. Gong, and S.-P. Ji, “Truncated peptides from Melittin and its analog with high lytic activity at endosomal pH enhance branched polyethylenimine-mediated gene transfection”, The Journal of Gene Medicine, vol. 14, 2012, pp. 241-250.

[22] J. Ivica, P. Williamson, and M. D. de Planque, “Salt gradient modulation of microRNA translocation through a biological nanopore”, Analytical Chemistry, vol. 89 (17), 2017, pp. 8822-8828.

[23] N. Saigo, K. Izumi, and R. Kawano, “Electrophysiological Analysis of Antimicrobial Peptides in Diverse Species”, ACS Omega, vol. 4, 2019, pp. 13124 – 13130.

[24] M. Laadhari, A. A. Arnold, A. E. Gravel, F. Separovic, and I. Marcotte, “Interaction of the antimicrobial peptides Caerin 1.1 and Aurein 1.2 with intact bacteria by ^{2}H solid-state NMR”, Biochimica et Biophysica Acta (BBA) – Biomembranes, vol. 1858 (12), 2016, pp. 2959-2964.

[25] P. Boland, and F. Separovic, “Membrane interactions of antimicrobial peptides from Australian tree frogs”, Biochimica et Biophysica Acta (BBA) – Biomembranes, vol. 1758 (9), 2006, pp. 1178-1183.

[26] D. I. Fernandez, J. D. Gehman, and F. Separovic, “Membrane interactions of antimicrobial peptides from Australian frogs”, Biochimica et Biophysica Acta (BBA) – Biomembranes, vol. 1788 (8), 2009, pp. 1630-1638.

[27] A. Mechler, S. Praporski, K. Atmuri, M. Boland, F. Separovic, and L. L. Martin, “Specific and Selective Peptide-Membrane Interactions Revealed Using Quartz Crystal Microbalance” Biophysical Journal, vol. 93 (11), 2007, pp. 3907-3916.

[28] D. I. Fernandez, A. P. Le Brun, T. C. Whitwell, M.-A. Sani, M. James, and F. Separovic, “The antimicrobial peptide Aurein 1.2 disrupts model membranes via the carpet mechanism”, Physical Chemistry Chemical Physics (PCCP), vol. 14 (45), 2012, pp. 15739-15751.

[29] R. Smith, F. Separovic, T. J. Milne, A. Whittaker, F. M. Bennet, B. A. Cornell, and A. Makriyannis, “Structure and orientation of the pore-forming peptide, melittin, in lipid bilayers”, Journal of Molecular Biology, vol. 241 (3), 1994, pp. 456-466.

[30] M.-A. Sani, and F. Separovic, “How Membrane-Active Peptides Get into Lipid Membranes”, Accounts of Chemical Research, vol. 49 (6), 2016, pp. 1130-1138.

[31] D. I. Fernandez, M.-A. Sani, A. J. Miles, B. A. Wallace, and F. Separovic, “Membrane defects enhance the interaction of antimicrobial peptides, Aurein 1.2 versus Caerin 1.1”, Biochimica et Biophysica Acta (BBA) – Biomembranes, vol. 1828 (8), 2013, pp. 1863-1872.

[32] D. Sengupta, H. Leontiadou, A. E. Mark, and S.-J. Marrink, “Toroidal pores formed by antimicrobial peptides show significant disorder”, Biochimica et Biophysica Acta (BBA) – Biomembranes, vol. 1778 (10), 2008, pp. 2308-2317.

[33] G. E. Balatti, M. F. Martini, and M. Pickholz, “A coarse-grained approach to studying the interactions of the antimicrobial peptides aurein 1.2 and maculatin 1.1 with POPG/POPE lipid mixtures”, Journal of Molecular Modeling, vol. 24 (8): 208, 2018.

[34] Y. Sun, T.-L. Sun, and H. W. Huang, “Mode of Action of Antimicrobial Peptides on *E. coli* Spheroplasts”, Biophysical Journal, vol. 111 (1), 2016, pp. 132-139.

[35] L. Yang, T. A. Harroun, T. M. Weiss, L. Ding, H. W. Huang, “Barrel-Stave Model or Toroidal Model? A Case Study on Melittin Pores”, Biophysical Journal, vol. 81 (3), 2001, pp. 1475-1485.

[36] G. van den Bogaart, J. V. Guzman, J. T. Mika, and B. Poolman, “On the Mechanism of Pore Formation by Melittin”, Journal of Biological Chemistry, vol. 283, 2008, pp. 33854-33857.

[37] N. Mookherjee, M. A. Anderson, H. P. Haagsman, and D. J. Davidson, “Antimicrobial host defence peptides: functions and clinical potential”, Nature Reviews Drug Discovery, vol. 19, 2020, pp. 311-322.

[38] Y. He and T. Lazaridis, “Activity Determinants of Helical Antimicrobial Peptides: A Large-Scale Computational Study”, PLoS ONE, vol. 8, 2013, e66440.

[39] N. Raheem and S. K. Straus, “Mechanisms of Action for Antimicrobial Peptides With Antibacterial and Antibiofilm Functions”, Frontiers in Microbiology, vol. 10, 2019, 2866.

[40] W. C. Wimley, “Describing the Mechanism of Antimicrobial Peptide Action with the Interfacial Activity Model”, ACS Chemical Biology, vol. 5, 2010, 905-917.

[41] A. H. Benfield and S. T. Henriques, “Mode-of-Action of Antimicrobial Peptides: Membrane Disruption vs. Intracellular Mechanisms”, Frontiers in Medical Technology, vol. 2, 2020, 610997.

[42] B. Bertrand, R. Garduño-Juárez, and C. Munoz-Garay, “Estimation of pore dimensions in lipid membranes induced by peptides and other biomolecules: A review”, Biochimica et Biophysica Acta (BBA) – Biomembranes, vol. 1863, 2021, 183551.

[43] Y. Sekiya, S. Sakashita, K. Shimizu, K. Usui, and R. Kawano, “Channel current analysis estimates the pore- formation and the penetration of transmembrane peptides”, Analyst, vol. 143, 2018, pp. 3540-3543.

[44] M. A. Czekalska, T. S. Kaminski, S. Jakiela, K. T. Sapra, H. Bayley and P. Garstecki “A droplet microfluidic system for sequential generation of lipid bilayers and transmembrane electrical recordings”, Lab on a Chip, vol. 15, 2015, pp. 541-548.

[45] R. Kawano, Y. Tsuji, K. Sato, T. Osaki, K. Kamiya, M. Hirano, T. Ide, N. Miki, and S. Takeuchi, “Automated Parallel Recordings of Topologically Identified Single Ion Channels”, Scientific Reports, vol. 3, 2013, 1995.